

LETTERS

p16^{INK4a} induces an age-dependent decline in islet regenerative potential

Janakiraman Krishnamurthy¹, Matthew R. Ramsey¹, Keith L. Ligon², Chad Torrice¹, Angela Koh³, Susan Bonner-Weir³ & Norman E. Sharpless¹

The p16^{INK4a} tumour suppressor accumulates in many tissues as a function of advancing age^{1–3}. p16^{INK4a} is an effector of senescence^{4,5} and a potent inhibitor of the proliferative kinase Cdk4 (ref. 6), which is essential for pancreatic β-cell proliferation in adult mammals^{7,8}. Here we show that p16^{INK4a} constrains islet proliferation and regeneration in an age-dependent manner. Expression of the p16^{INK4a} transcript is enriched in purified islets compared with the exocrine pancreas, and islet-specific expression of p16^{INK4a}, but not other cyclin-dependent kinase inhibitors, increases markedly with ageing. To determine the physiological significance of p16^{INK4a} accumulation on islet function, we assessed the impact of p16^{INK4a} deficiency and overexpression with increasing age and in the regenerative response after exposure to a specific β-cell toxin. Transgenic mice that over-express p16^{INK4a} to a degree seen with ageing demonstrated decreased islet proliferation. Similarly, islet proliferation was unaffected by p16^{INK4a} deficiency in young mice, but was relatively increased in p16^{INK4a}-deficient old mice. Survival after toxin-mediated ablation of β-cells, which requires islet proliferation, declined with advancing age; however, mice lacking p16^{INK4a} demonstrated enhanced islet proliferation and survival after β-cell ablation. These genetic data support the view that an age-induced increase of p16^{INK4a} expression limits the regenerative capacity of β-cells with ageing.

Mammalian homeostasis depends on the function of reservoirs of proliferating cells necessary for tissue regeneration, and therefore regulators of proliferation are thought to be involved in ageing^{4,5}. In particular, p16^{INK4a}, a product of the INK4a/ARF (*Cdkn2a*) locus, has been postulated to contribute to ageing. Although its expression increases with age in most tissues^{1–3}, we chose to study its role in the pancreatic islet for several reasons. Expression of p16^{INK4a} sharply increases with ageing in the endocrine pancreas of rodents and humans^{2,3}. Cultured human islets undergo telomere-independent senescence in the setting of p16^{INK4a} induction⁹, suggesting that p16^{INK4a} can be a principal mediator of proliferation in this cell type. Mice lacking Cdk4 or cyclin D1/2, which activate Cdk4, are born with normal islet mass, but develop diabetes in the setting of reduced proliferation and islet mass as young adults^{7,8,10}. Mice with increased islet Cdk4 activity, because of p18^{INK4c} deficiency or activating mutations of Cdk4 (refs 11–13), show an increase in islet mass. Therefore, the islet seems to be an ideal compartment for determining the consequences of p16^{INK4a}, as expression increases with ageing in this tissue, and the principal biochemical target of p16^{INK4a} has a clear role in β-cell proliferation.

To define the compartmental and age-related expression of p16^{INK4a}, we isolated islets from total pancreas as described¹⁴. Total

RNA was harvested from islets and exocrine pancreas from 12–14-week-old and 64–80-week-old mice, and the expression of indicated transcripts determined by quantitative TaqMan analysis (Fig. 1a, b and Supplementary Fig. 1). Using this approach, we detected p16^{INK4a} expression in the islets of young animals, which increased by 14-fold (mean value) with 52–66 weeks of additional ageing. Expression of p16^{INK4a} was enriched in purified islets, with >30-fold higher expression than in the exocrine pancreas. As is the case in most rodent tissues^{1,2}, expression of Arf, the other *Ink4a/Arf* transcript, mirrored p16^{INK4a}, with a similar degree of age-induced increase and islet enrichment. However, the messenger RNA expression of other cyclin-dependent kinase inhibitors in this compartment changed only modestly or not at all with ageing (Fig. 1b and Supplementary

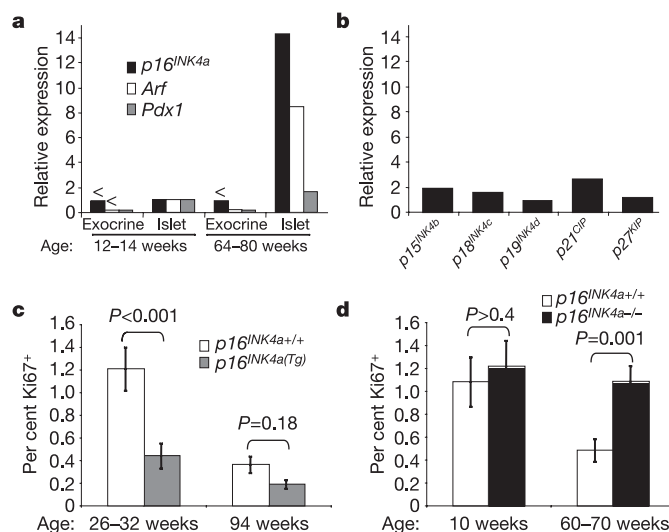


Figure 1 | Islet gene expression and proliferation in young versus old mice. **a**, Expression of p16^{INK4a}, Arf and Pdx1 as determined by TaqMan on islets and exocrine pancreas from mice of indicated ages. Relative expression is shown normalized to islet expression in young mice. ‘<’ indicates expression beneath the lower limit of detection. **b**, Relative mRNA expression of the indicated genes in islets with ageing. Values are reported as mean ratio of expression in old (64–80 weeks) versus young (12–14 weeks) mice. **c**, Per cent Ki67-positive cells of pancreatic islets from p16^{INK4a} wild-type and overexpressing BAC transgenic mice of indicated ages. Error bars indicate \pm s.e.m.; *P*-values were determined by Mann–Whitney *U*-test. **d**, Per cent Ki67-positive cells of pancreatic islets from p16^{INK4a}+/+ and p16^{INK4a}-/- mice of indicated ages. Error bars indicate \pm s.e.m.; *P*-values were determined by Mann–Whitney *U*-test.

¹Departments of Medicine and Genetics, The Lineberger Comprehensive Cancer Center, The University of North Carolina School of Medicine, Chapel Hill, North Carolina 27599, USA. ²Department of Pathology, Brigham and Women's Hospital and Harvard Medical School, Boston, Massachusetts 02115, USA. ³Joslin Diabetes Center and Harvard Medical School, Boston, Massachusetts 02115, USA.

Fig. 1). Notably, both products of the *Ink4a/Arf* locus were more enriched in the islet than *Pdx1* (Fig. 1a), a transcription factor mainly restricted to β -cells in adults¹⁵. These data demonstrate that islet expression of the *Ink4a/Arf* locus is comparable to that seen in other highly expressing tissues such as spleen or lung² and sharply increases with ageing. Moreover, although other cell cycle inhibitors such as p18^{INK4c} and p27^{KIP1} have a more important role in determining β -cell proliferation and number during development and young adulthood^{13,16}, the marked transcriptional increase with ageing seems to be a unique property among cell cycle inhibitors of the products of the *Ink4a/Arf* locus.

We did not detect a difference in either the total number of cells or the number of proliferating cells per islet in young *p16^{INK4a}*-deficient animals compared to controls. To test whether an increase in *p16^{INK4a}* level comparable to that seen with ageing (Fig. 1a) would regulate islet proliferation, we generated *p16^{INK4a}* bacterial artificial chromosome (BAC) transgenic mice harbouring a single extra copy of the *p16^{INK4a}* gene (Supplementary Fig. 2). We identified a line (*p16^{INK4a(Tg)}*) that demonstrated a mean fivefold increase in expression of *p16^{INK4a}* mRNA and protein across a panel of tissues including the pancreas (Supplementary Figs 2 and 3). In young transgenic mice, *p16^{INK4a}* expression was comparable to that in ~60-week-old wild-type mice. Transgenic animals demonstrated normal size, fertility and glucose metabolism (not shown). A reduction in proliferation was noted in islets from *p16^{INK4a(Tg)}* mice compared to littermate controls at all ages, but the effect was greatest in young mice (Fig. 1c). This observation suggests that the level of *p16^{INK4a}* expression detected in ~60-week-old animals inhibits islet proliferation.

To determine the effects of endogenous *p16^{INK4a}* with ageing, islet proliferation in young and old *p16^{INK4a+/+}* and *p16^{INK4a-/-}* mice was analysed (Fig. 1d). No evidence of pancreatic neoplasia was

noted in *p16^{INK4a}*-deficient animals, and germline deficiency of *p16^{INK4a}* did not influence weight in mice less than a year of age (Supplementary Fig. 4). Islet proliferation measured by calculating the Ki67⁺ proliferation index significantly decreased with ageing in *p16^{INK4a+/+}* mice (from 1.21% of islet cells in 20-week-old mice to 0.36% of cells in 94-week-old mice; $P < 0.001$ for trend, Fig. 1c, d). Although germline *p16^{INK4a}* inactivation did not affect islet proliferation in young mice, the age-induced decrease in proliferation was largely rescued by *p16^{INK4a}* deficiency (Fig. 1d). We believe that complete rescue of islet proliferation is not noted in *p16^{INK4a-/-}* mice because these animals demonstrate unperturbed *Arf* expression, which also increases with ageing in this tissue (Fig. 1a and not shown), as well as the possible existence of *Ink4a/Arf*-independent mechanisms of ageing. In aggregate, the results from the BAC transgenic and germline knockout strains demonstrate that with ageing, *p16^{INK4a}* expression becomes a significant regulator of islet proliferation.

The tumour-prone nature^{17,18} of *p16^{INK4a}*-deficient animals limited our ability to determine the functional significance of this inhibition of proliferation imposed by *p16^{INK4a}* with ageing. For example, assays of glucose tolerance even in mice of intermediate age (40–52 weeks old) were confounded by initially undetected tumours in the *p16^{INK4a-/-}* cohort (Supplementary Fig. 4). Thus, to study the effect of *p16^{INK4a}* expression on islet function in young adult animals, we adopted a model of islet regeneration after treatment with streptozotocin (STZ). STZ is a specific β -cell toxin that induces necrosis and diabetes when given as a single dose to adult mice, and moderate β -cell regeneration after STZ treatment is well described^{19–21}. After determining a STZ dose (150 mg kg⁻¹) that led to death from diabetes within 100 days of injection in ~75% of 10-week-old C57BL/6 mice, we harvested and analysed pancreata at indicated times after STZ injection. Islet proliferation was signifi-

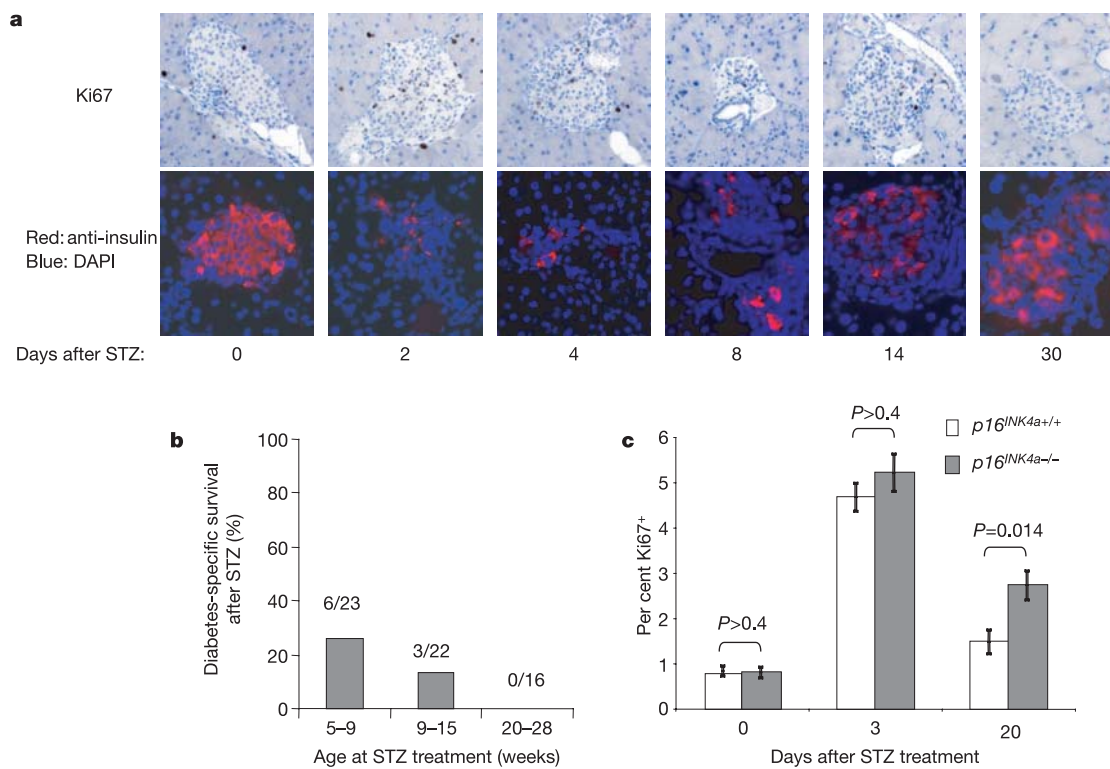


Figure 2 | Islet regeneration after STZ treatment. **a**, Ki67 immunohistochemistry and anti-insulin/DAPI immunofluorescence taken at indicated times after STZ treatment. Original magnification, $\times 200$. **b**, Survival of wild-type C57BL/6 mice after STZ treatment by age on the day of STZ injection. Acute STZ deaths (within 5 days of treatment) are censored from

the analysis. Total numbers of long-term (>100 days after STZ) survivors over total number of mice treated per age are indicated. **c**, Per cent Ki67⁺ positive cells of pancreatic islets from 33-week-old *p16^{INK4a+/+}* and *p16^{INK4a-/-}* mice at indicated time points after STZ treatment. Error bars indicate \pm s.e.m.; P -values were determined by Mann–Whitney *U*-test.

cantly increased 2 days after STZ treatment, and remained elevated for 2 weeks after STZ treatment (Supplementary Fig. 5). Double-labelling with Ki67 and insulin demonstrated that >80% of proliferating cells in the islets of untreated mice or after STZ treatment were β -cells, suggesting that islet proliferation and β -cell proliferation strongly correlate in this system.

Islets were depleted of β -cells at 2 and 4 days after STZ treatment, although median cell number per islet did not reach its lowest point until 8 days after STZ treatment (Fig. 2a and Supplementary Fig. 5). At this time point, small, insulin-positive islets associated with ducts were evident, with increasing islet size and insulin expression 14 and 30 days after STZ treatment. Mice surviving more than 30 days after STZ treatment demonstrated a partial recovery of islet size relative to pre-treatment levels. All mice surviving 100 days after STZ treatment showed recovery of β -cell function as demonstrated by resolution of hyperglycaemia and weight gain in excess of pre-treatment weight

(Fig. 3a–c). Notably, islet regeneration after STZ treatment was age dependent (Fig. 2b). Greater than 25% of 5–9-week-old wild-type mice survived more than 100 days after STZ treatment, whereas no wild-type animal older than 20 weeks demonstrated survival after STZ ($P = 0.026$). This does not reflect increased sensitivity to STZ in older cohorts, as old adult mice have been shown to be less sensitive to the β -cell-damaging effects of STZ²⁰. These data suggest that prolonged survival after a single diabetes-causing dose of STZ requires regeneration of significant numbers of functional β -cells, an ability that declines with ageing.

To determine whether $p16^{INK4a}$ expression contributes to the age-dependent decline in β -cell regeneration, we performed STZ challenge in littermate cohorts of animals of indicated ages. Mice were treated with STZ, and followed serially for islet proliferation (Fig. 2c), weight (Fig. 3a), serum glucose levels (Fig. 3b, c) and diabetes-specific survival (Fig. 4a–c). In 33-week-old STZ-treated mice, islet proliferation was similar in $p16^{INK4a+/+}$ and $p16^{INK4a-/-}$ mice before and 3 days after treatment. A significant increase in proliferation, however, was noted in $p16^{INK4a-/-}$ mice at 20 days after STZ treatment (Fig. 2c). This effect, only at the later time point after islet ablation, probably reflects a delayed (>2 weeks) induction of $p16^{INK4a}$ expression after a DNA damaging stimulus, as has been described in other systems^{22–25}. These data indicate that $p16^{INK4a}$ expression limits islet proliferation after β -cell depletion by STZ.

Survival was measured to determine whether differences in islet proliferation after STZ treatment translated into benefit for $p16^{INK4a}$ -deficient animals. No effect of $p16^{INK4a}$ deficiency on STZ toxicity was noted in 5–9-week-old mice (Fig. 4a), but

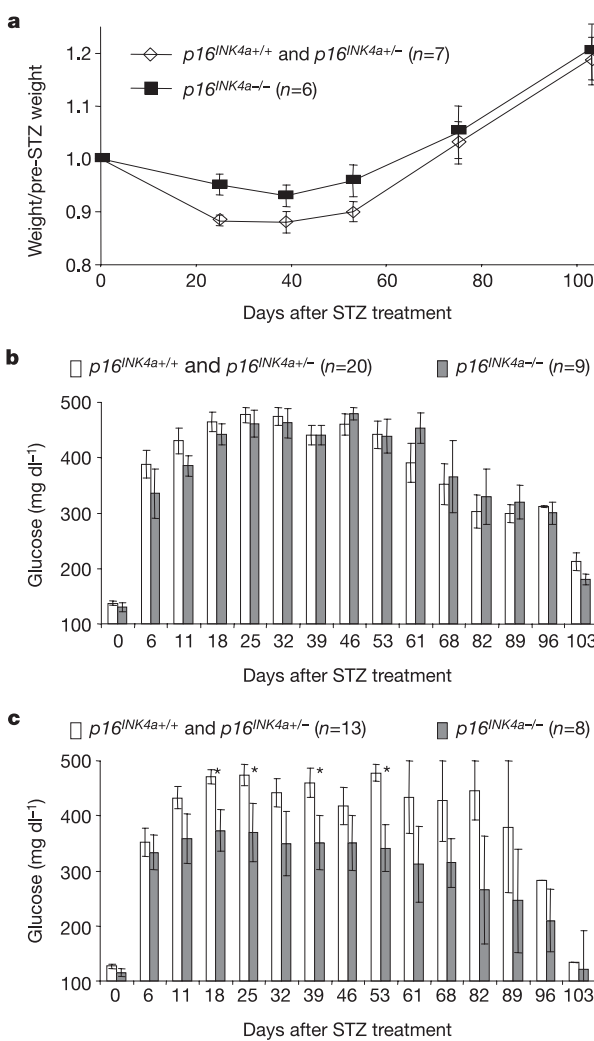


Figure 3 | Metabolic effects of $p16^{INK4a}$ expression after STZ treatment. **a**, Animal weight after STZ treatment normalized to pre-treatment weight of long-term (>100 days) surviving mice (5–28 weeks of age) by indicated genotypes. All long-term surviving animals showed improved hyperglycaemia and began to regain weight within 55 days after STZ treatment, regardless of genotype. Error bars indicate \pm s.e.m. **b, c**, Fasting serum glucose levels after STZ treatment. No difference in fasting serum glucose or survival was seen in mice less than 9 weeks of age after STZ treatment (**b**), but hyperglycaemia was more marked and persistent after STZ treatment in mice greater than 9 weeks of age (9–15 weeks) (**c**). Results are shown \pm s.e.m.; asterisks indicate $P < 0.05$ on the indicated days as determined by two-sided *t*-test.

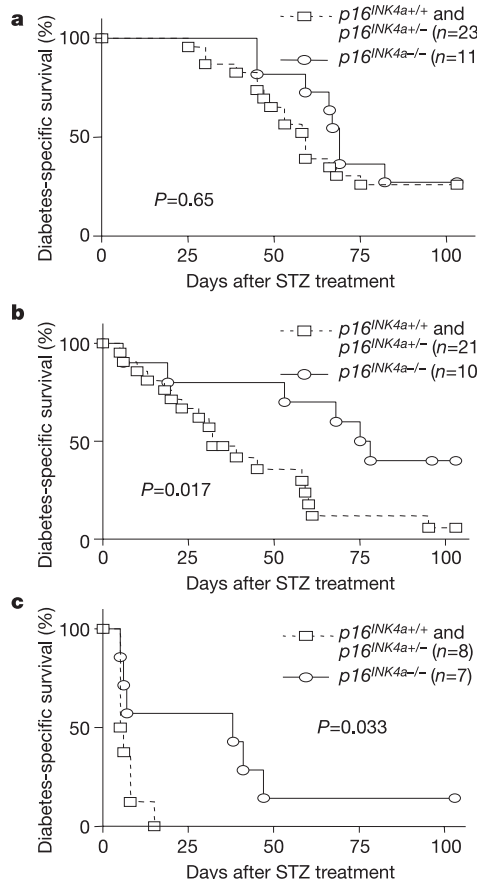


Figure 4 | Influence of $p16^{INK4a}$ expression on islet regeneration after STZ treatment. **a–c**, Diabetes-specific survival after STZ treatment of mice treated at 5–9 weeks (**a**), 9–15 weeks (**b**) or 20–28 weeks (**c**) of age. Indicated P -values were determined by log-rank test.

p16^{INK4a} deficiency afforded resistance to STZ in older animals (Fig. 4b, c). After STZ injection, older *p16^{INK4a-/-}* animals exhibited a more rapid recovery to pre-treatment weight (Fig. 3a), a higher probability of return to normo-glycaemia (Fig. 3c), and enhanced survival (Fig. 4b, c) compared with *p16^{INK4a+/+}* littermates. Although the greatest survival differences were seen in the oldest mice, as with islet proliferation, *p16^{INK4a}* deficiency did not entirely rescue this age-induced phenotype. Therefore, an age-associated increase in *p16^{INK4a}* expression seems to limit the recovery of islet function after STZ ablation, but *p16^{INK4a}*-independent mechanism(s) of islet ageing also seem to exist.

These data suggest that *p16^{INK4a}* mediates a decline in the replicative capacity of islets associated with ageing and, in this compartment, is both a biological marker and effector of ageing. Several lines of evidence support the notion that *p16^{INK4a}* expression also contributes to ageing in additional tissues. The expression of *p16^{INK4a}* in most mammalian tissues strongly correlates with ageing¹ and in some tissues is attenuated by caloric restriction², which retards mammalian ageing. Furthermore, increased expression of *p16^{INK4a}* with ageing diminishes the replicative capacities of neural and haematopoietic stem cells in a cell-autonomous fashion^{26,27}. These results from diverse systems suggest that *p16^{INK4a}* contributes to mammalian ageing by limiting the self-renewal of regenerative cells in at least the bone marrow, brain and endocrine pancreas.

Although expression of *p16^{INK4a}* has an age-dependent impact on islet proliferation and regeneration, the compartment in which *p16^{INK4a}* exerts an age-promoting function is not clear. The simplest model would be that *p16^{INK4a}* expression in β -cells directly limits their replication, which has been suggested to be the principal mechanism of β -cell production in adult mice²⁸. Alternatively, *p16^{INK4a}* could regulate the proliferation of putative stem cells suggested to contribute to β -cell production in adult mice²⁹. It is also not clear how inhibition of cyclin D/Cdk4 activity by *p16^{INK4a}* exerts an age-promoting function. It is possible that *p16^{INK4a}* induces an irreversible growth arrest (senescence) of β -cells or their progenitors, as has been suggested previously³⁰. Alternatively, it is possible that *p16^{INK4a}* expression decreases the frequency of cell cycle entry without inducing a permanent growth arrest.

Although insulin resistance is a characteristic feature of type 2 diabetes mellitus, most adults with insulin resistance do not develop type 2 diabetes mellitus. Similarly, the sharp increase in the incidence of type 2 diabetes mellitus with age cannot be solely attributed to increased insulin resistance. Recent evidence has demonstrated a decrease in β -cell mass of type 2 diabetes mellitus patients relative to matched non-diabetic controls^{31,32}. Our data indicate that increased *p16^{INK4a}* expression with ageing contributes to a relative failure of islet proliferation. This observation suggests the possibility that type 2 diabetes mellitus, in part, results from a *p16^{INK4a}*-induced replicative failure of islets with ageing. Further studies, however, are required to link formally senescence and type 2 diabetes mellitus in humans.

METHODS

Islets and exocrine pancreas were isolated from C57BL/6 mice (Jackson Labs) of indicated ages as described¹⁴. TaqMan analysis was performed as described² with minor modifications described in Supplementary Methods. Single-copy BAC transgenic mice overexpressing *p16^{INK4a}* but not *Arf* or *p15^{INK4b}* were generated using a 64-kilobase genomic clone derived from the RPCI-22 (129/SvEv) BAC library. Eleven independent founder lines were generated, at least two of which were single-copy integrants (Supplementary Fig. 2). All experiments were performed using littermate progeny from a single-copy transgenic line (*p16^{INK4a(Tg)}*) demonstrating mean ~5-fold overexpression of *p16^{INK4a}* mRNA and protein across a panel of tissues (Supplementary Figs 2 and 3). Islet proliferation and STZ survival experiments were performed in littermate progeny from *p16^{INK4a-/-}* intercrosses in the C57BL/6 and FVB/n backgrounds (see Supplementary Methods). For survival after STZ treatment, cohorts of littermate mice of indicated genotypes were treated with STZ (150 mg kg⁻¹ body weight). Comparisons of proliferation were performed by calculation of the Ki67 proliferative index using established methods within the Brigham and

Women's Hospital Pathology Immunohistochemical Laboratory. Insulin staining and Ki67/insulin double staining were performed as described in Supplementary Information. Detailed methodological information is available in Supplementary Methods.

Received 11 April; accepted 24 July 2006.

Published online 6 September 2006.

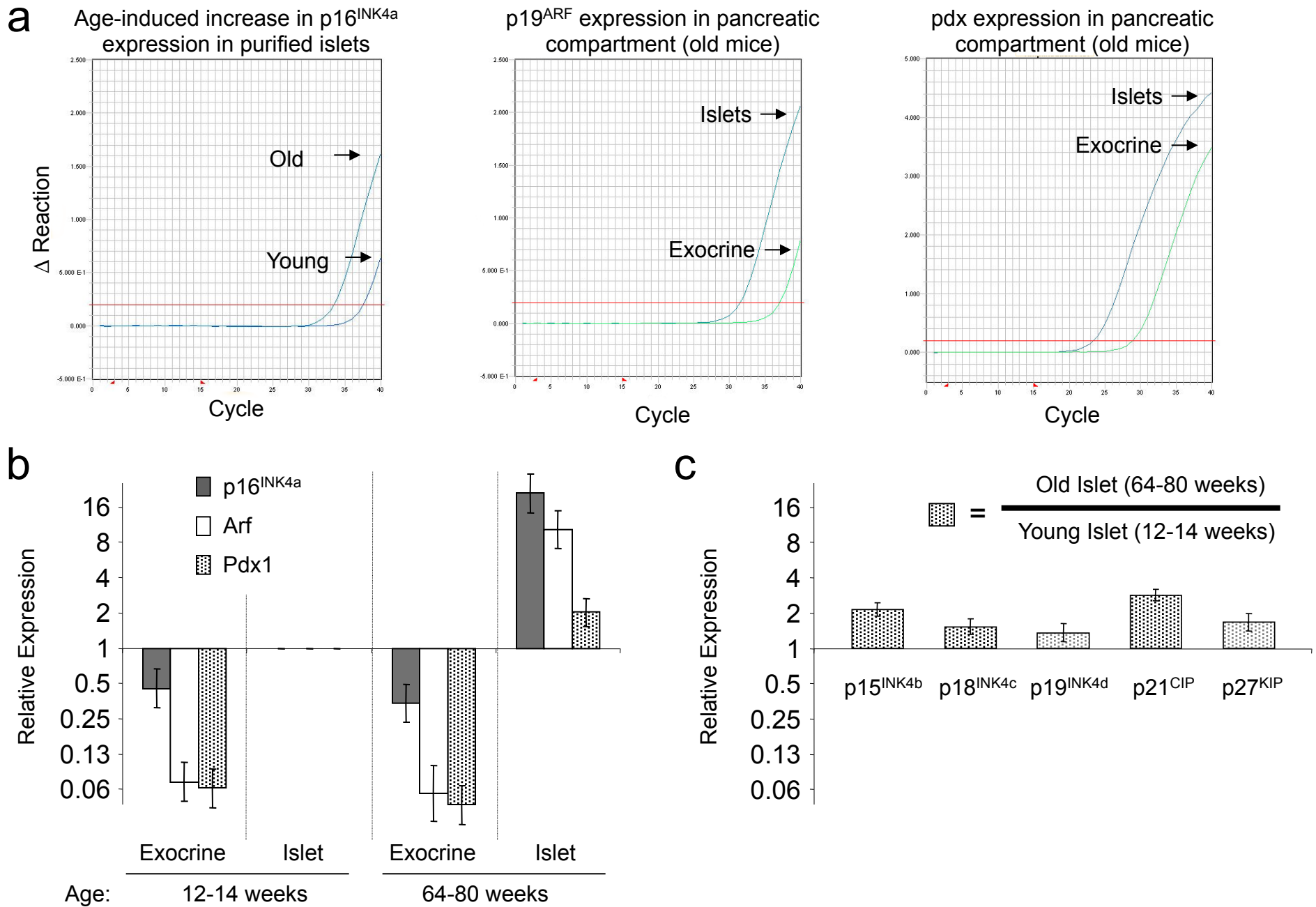
- Zindy, F., Quelle, D. E., Roussel, M. F. & Sherr, C. J. Expression of the *p16^{INK4a}* tumor suppressor versus other INK4 family members during mouse development and aging. *Oncogene* 15, 203–211 (1997).
- Krishnamurthy, J. et al. *Ink4a/Arf* expression is a biomarker of aging. *J. Clin. Invest.* 114, 1299–1307 (2004).
- Nielsen, G. P. et al. Immunohistochemical survey of *p16^{INK4a}* expression in normal human adult and infant tissues. *Lab. Invest.* 79, 1137–1143 (1999).
- Park, I. K., Morrison, S. J. & Clarke, M. F. Bmi1, stem cells, and senescence regulation. *J. Clin. Invest.* 113, 175–179 (2004).
- Campisi, J. Cancer and ageing: rival demons? *Nature Rev. Cancer* 3, 339–349 (2003).
- Lowe, S. W. & Sherr, C. J. Tumor suppression by *Ink4a-Arf*: progress and puzzles. *Curr. Opin. Genet. Dev.* 13, 77–83 (2003).
- Rane, S. G. et al. Loss of Cdk4 expression causes insulin-deficient diabetes and Cdk4 activation results in β -islet cell hyperplasia. *Nature Genet.* 22, 44–52 (1999).
- Tsutsui, T. et al. Targeted disruption of CDK4 delays cell cycle entry with enhanced p27^{Kip1} activity. *Mol. Cell. Biol.* 19, 7011–7019 (1999).
- Halvorsen, T. L., Beattie, G. M., Lopez, A. D., Hayek, A. & Levine, F. Accelerated telomere shortening and senescence in human pancreatic islet cells stimulated to divide *in vitro*. *J. Endocrinol.* 166, 103–109 (2000).
- Kushner, J. A. et al. Cyclins D2 and D1 are essential for postnatal pancreatic β -cell growth. *Mol. Cell. Biol.* 25, 3752–3762 (2005).
- Hino, S. et al. *In vivo* proliferation of differentiated pancreatic islet β cells in transgenic mice expressing mutated cyclin-dependent kinase 4. *Diabetologia* 47, 1819–1830 (2004).
- Marzo, N. et al. Pancreatic islets from cyclin-dependent kinase 4/R24C (Cdk4) knockin mice have significantly increased β cell mass and are physiologically functional, indicating that Cdk4 is a potential target for pancreatic β cell mass regeneration in Type 1 diabetes. *Diabetologia* 47, 686–694 (2004).
- Pei, X. H., Bai, F., Tsutsui, T., Kiyokawa, H. & Xiong, Y. Genetic evidence for functional dependency of *p18^{Ink4c}* on Cdk4. *Mol. Cell. Biol.* 24, 6653–6664 (2004).
- Montana, E., Bonner-Weir, S. & Weir, G. C. Beta cell mass and growth after syngeneic islet cell transplantation in normal and streptozocin diabetic C57BL/6 mice. *J. Clin. Invest.* 91, 780–787 (1993).
- Fernandes, A. et al. Differentiation of new insulin-producing cells is induced by injury in adult pancreatic islets. *Endocrinology* 138, 1750–1762 (1997).
- Uchida, T. et al. Deletion of *Cdkn1b* ameliorates hyperglycemia by maintaining compensatory hyperinsulinemia in diabetic mice. *Nature Med.* 11, 175–182 (2005).
- Sharpless, N. E. et al. Loss of *p16^{Ink4a}* with retention of *p19^{Arf}* predisposes mice to tumorigenesis. *Nature* 413, 86–91 (2001).
- Sharpless, N. E., Ramsey, M. R., Balasubramanian, P., Castrillon, D. H. & DePinho, R. A. The differential impact of *p16^{INK4a}* or *p19^{Arf}* deficiency on cell growth and tumorigenesis. *Oncogene* 23, 379–385 (2004).
- Bonner-Weir, S., Trent, D. F., Honey, R. N. & Weir, G. C. Responses of neonatal rat islets to streptozotocin: limited β -cell regeneration and hyperglycemia. *Diabetes* 30, 64–69 (1981).
- Riley, W. J., McConnell, T. J., Maclare, N. K., McLaughlin, J. V. & Taylor, G. The diabetogenic effects of streptozotocin in mice are prolonged and inversely related to age. *Diabetes* 30, 718–723 (1981).
- Gu, D., Arnush, M. & Sarvetnick, N. Endocrine/exocrine intermediate cells in streptozotocin-treated *Ins-IFN- γ* transgenic mice. *Pancreas* 15, 246–250 (1997).
- Meng, A., Wang, Y., Van Zant, G. & Zhou, D. Ionizing radiation and busulfan induce premature senescence in murine bone marrow hematopoietic cells. *Cancer Res.* 63, 5414–5419 (2003).
- Wang, Y., Schulte, B. A., Larue, A. C., Ogawa, M. & Zhou, D. Total body irradiation selectively induces murine hematopoietic stem cell senescence. *Blood* 107, 358–366 (2006).
- Jacobs, J. J. & de Lange, T. Significant role for *p16^{INK4a}* in p53-independent telomere-directed senescence. *Curr. Biol.* 14, 2302–2308 (2004).
- Robles, S. J. & Adam, G. R. Agents that cause DNA double strand breaks lead to *p16^{INK4a}* enrichment and the premature senescence of normal fibroblasts. *Oncogene* 16, 1113–1123 (1998).
- Molofsky, A. V. et al. Increasing *p16^{INK4a}* expression decreases forebrain progenitors and neurogenesis during ageing. *Nature advance* online publication, doi:10.1038/nature05091 (6 September 2006).
- Janzen, V. et al. Stem-cell ageing modified by the cyclin-dependent kinase inhibitor *p16^{INK4a}*. *Nature advance* online publication, doi:10.1038/nature05159 (6 September 2006).
- Dor, Y., Brown, J., Martinez, O. I. & Melton, D. A. Adult pancreatic β -cells are formed by self-duplication rather than stem-cell differentiation. *Nature* 429, 41–46 (2004).

29. Bonner-Weir, S. & Weir, G. C. New sources of pancreatic β -cells. *Nature Biotechnol.* **23**, 857–861 (2005).
30. Sone, H. & Kagawa, Y. Pancreatic β cell senescence contributes to the pathogenesis of type 2 diabetes in high-fat diet-induced diabetic mice. *Diabetologia* **48**, 58–67 (2005).
31. Butler, A. E. *et al.* β -cell deficit and increased β -cell apoptosis in humans with type 2 diabetes. *Diabetes* **52**, 102–110 (2003).
32. Yoon, K. H. *et al.* Selective β -cell loss and α -cell expansion in patients with type 2 diabetes mellitus in Korea. *J. Clin. Endocrinol. Metab.* **88**, 2300–2308 (2003).

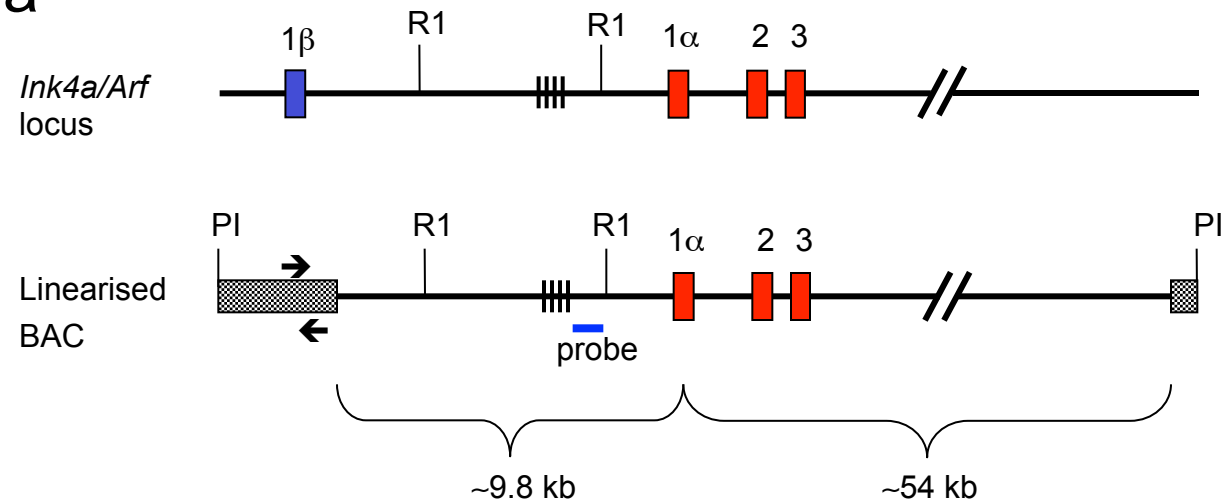
Supplementary Information is linked to the online version of the paper at www.nature.com/nature.

Acknowledgements We thank J. Lock, S. Alson, M. Zhang, Y. Xiong and G. Enders for advice, reagents and technical support, and R. DePinho and K. Wong for comments on the manuscript. This work was supported by grants from the Sidney Kimmel Cancer Foundation for Cancer Research, the Paul Beeson Physician Scholars program, the Ellison Medical Foundation, and the National Institutes of Health.

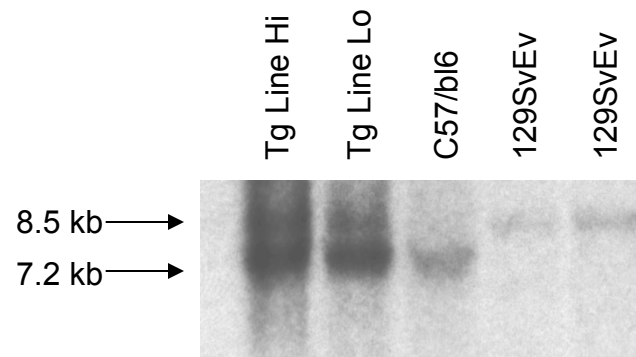
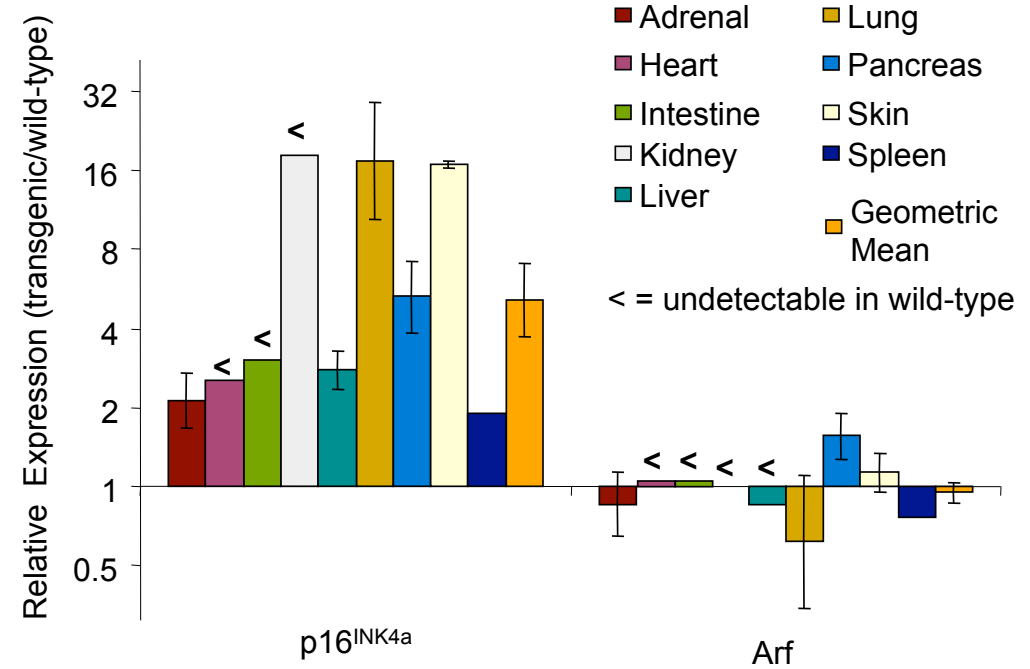
Author Information Reprints and permissions information is available at www.nature.com/reprints. The authors declare no competing financial interests. Correspondence and requests for materials should be addressed to N.E.S. (NES@med.unc.edu).

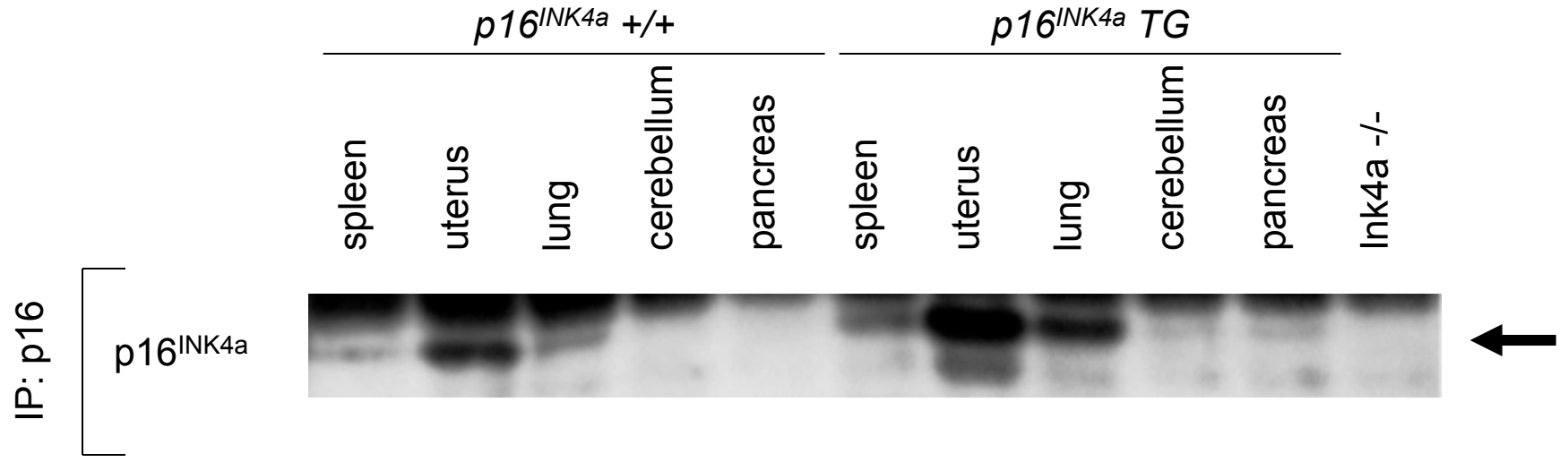


Krishnamurthy et al., Supp. Figure 1

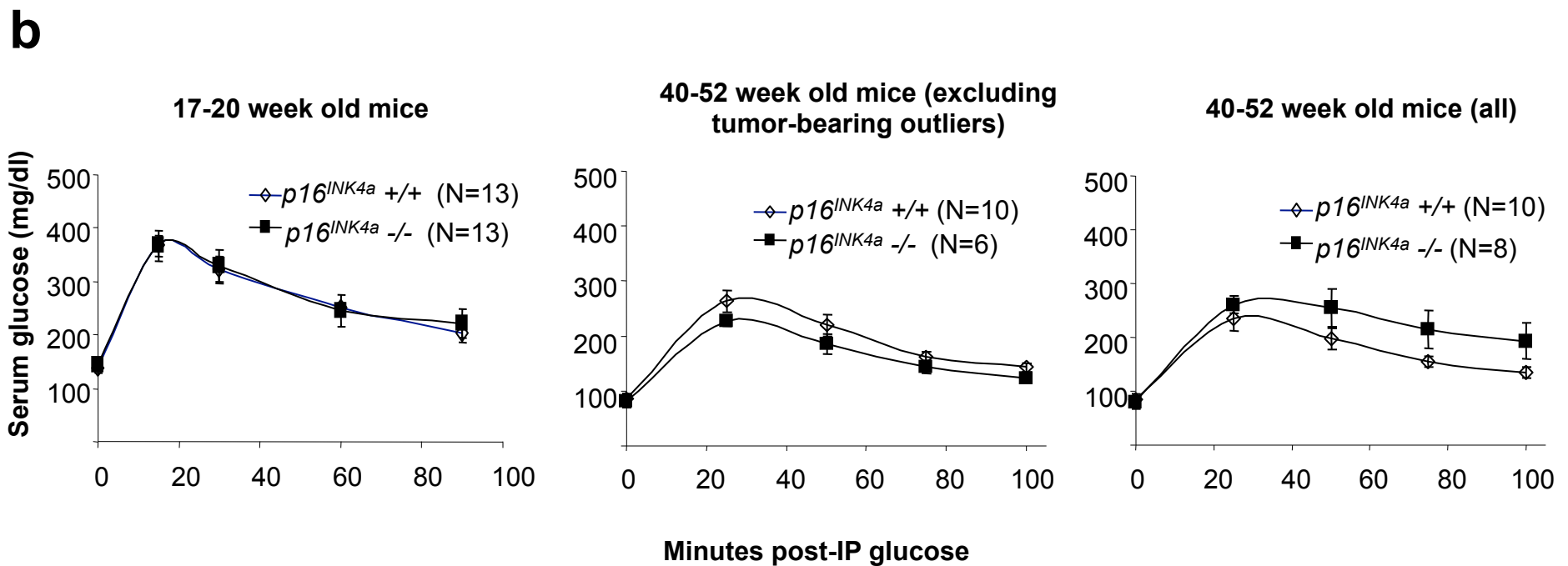
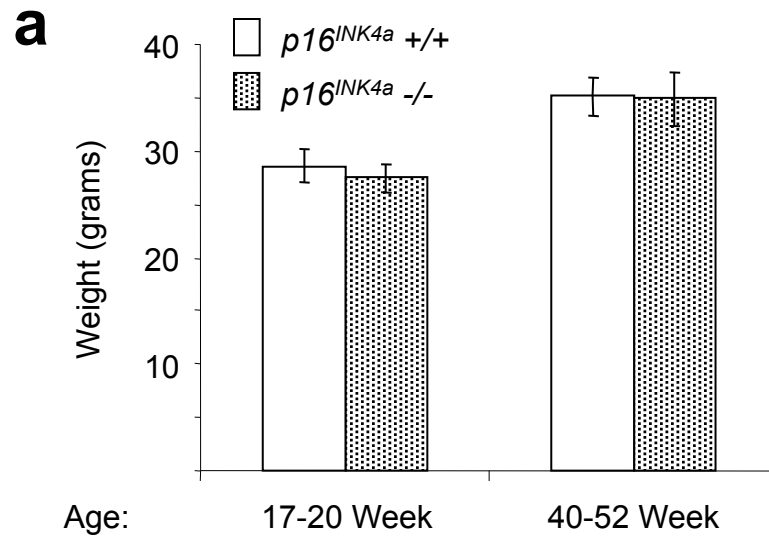
a

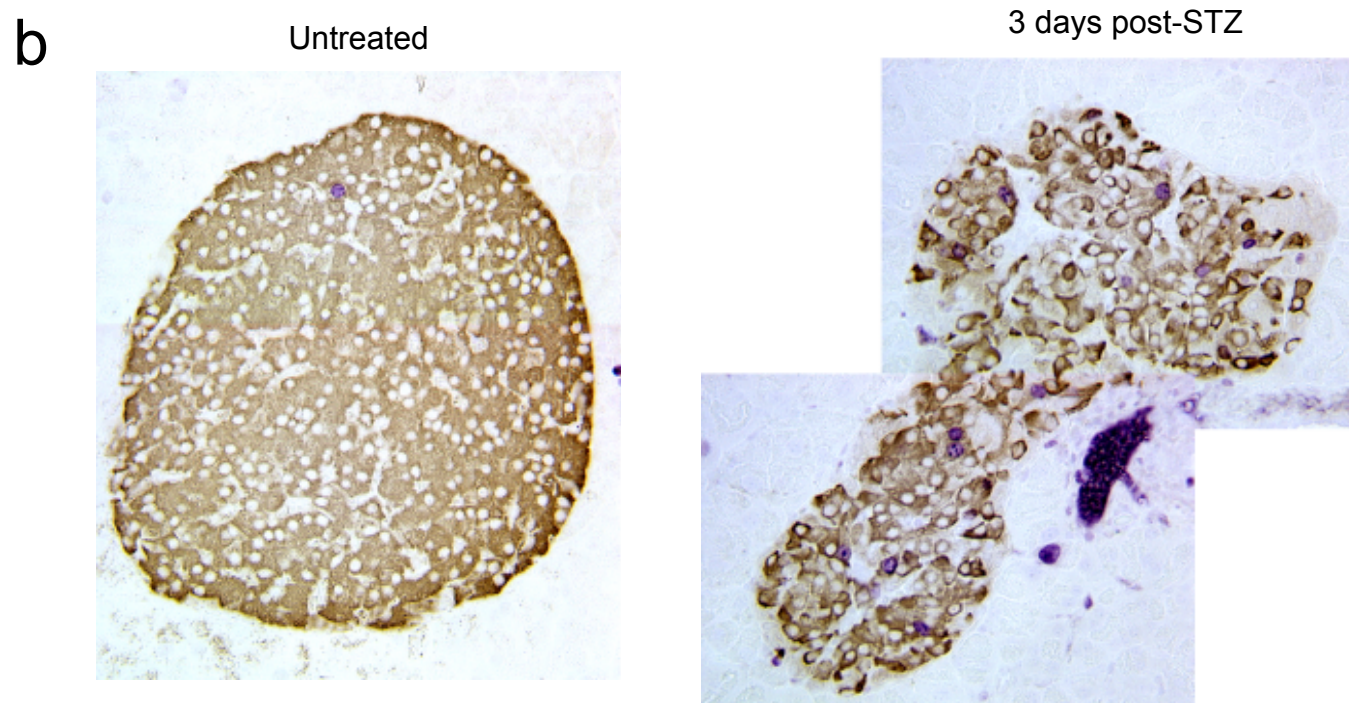
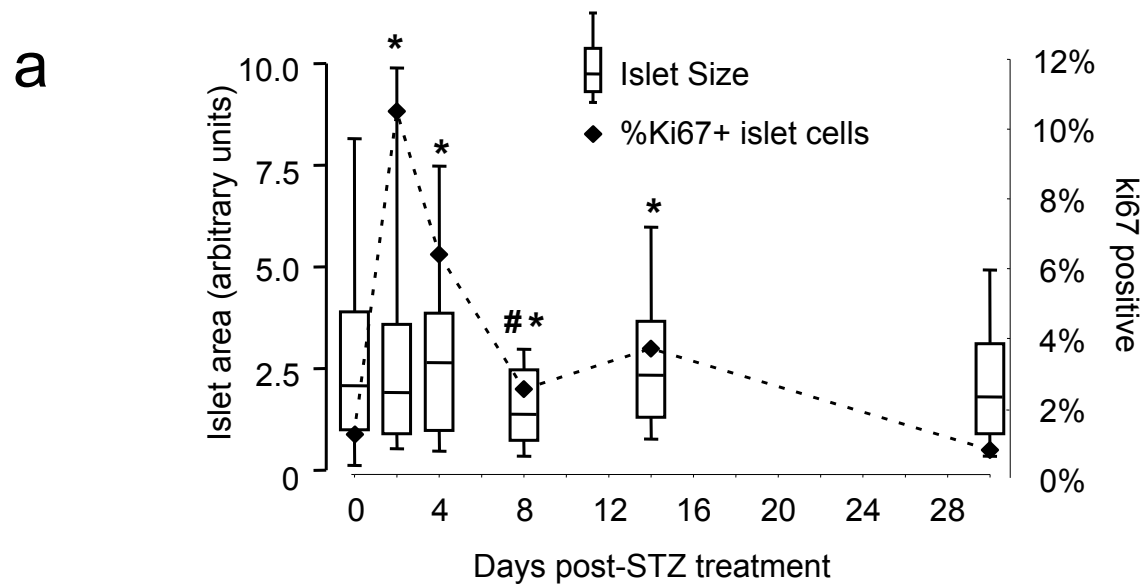
- PI = Intron encoded nuclease
- PI-SceI
- RI = Eco RI
- III = Variable microsatellite region
- ← = PCR screening primers

b**c**



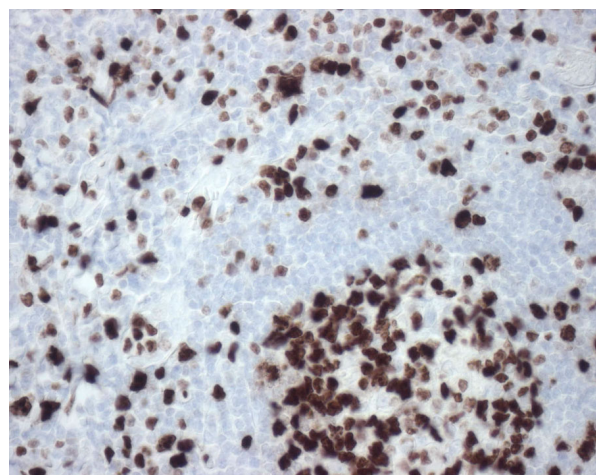
Krishnamurthy et al., Supp. Figure 3



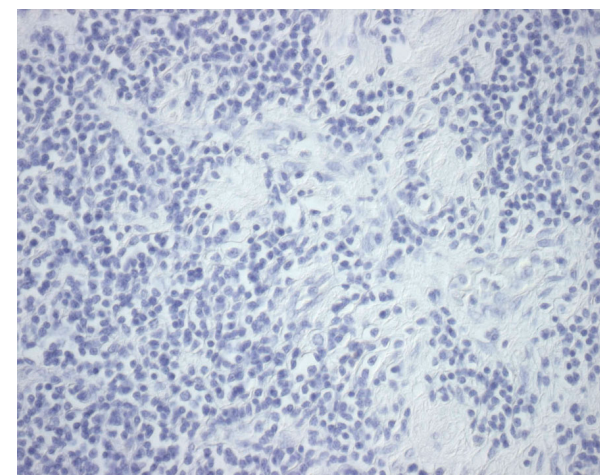


Krishnamurthy et al., Supp. Figure 5

tonsil



appendix



Ki67 = brown stain

Supplemental Methods:

BAC Transgenics and knockout mice: An RPCI-22 mouse BAC library (<http://bacpac.chori.org/mouse22.htm>) was screened using a *p16^{INK4a}* probe (RsaI & AccI fragment, 2.5 kb upstream to the ATG site) and a 64 Kb genomic clone containing exon 1 α , exon 2 and exon 3 (of *p16^{INK4a}*), but not exon 1 β (of ARF) or exons of *p15^{INK4b}*, was identified. For generating transgenic mice, purified BAC was linearised and injected into fertilized (C57/Bl6 X C3H) eggs at the UNC Animal Models Core Facility . Transgenic founders were detected by PCR primers specific for the vector region and by Southern blotting. By Southern analysis, the transgenic allele (129/SvEv) could be distinguished from the endogenous C57Bl/6 allele because of a known restriction fragment length polymorphism in the *p16^{INK4a}* promoter region between these two strains, permitting identification of single copy integrants. Eleven independent founder lines were generated, at least two of which were single copy integrants (Supplemental Figure 2). All experiments described in this work were performed using littermate progeny from a single-copy integrant transgenic line (*p16^{INK4a} TG*) demonstrating mean ~5-fold overexpression of *p16^{INK4a}* as determined by TaqMan in representative tissues from 26- and 84-week old mice and by IP-Western blotting (Supplemental Figures 2 and 3). For IP-Western blotting, tissues were homogenized and lysed in RIPA buffer (200mM Tris -HCl pH 7.4, 130mM NaCl, 10% glycerol, 0.5% SDS, 1% Triton-X 100, 0.5% sodium deoxycholate). Three mg of total protein was pre-cleared with 50 μ l Protein A agarose beads (Invitrogen), and cleared lysate was incubated overnight at 4°C with 2 μ g *p16^{INK4a}* antibody (M-156, Santa Cruz). Lysate was incubated with protein A beads for 2 hours at 4°C. Protein was separated on a 4-12% Bis-Tris mini-gel (Invitrogen) and transferred to Immobilon-P membrane (Millipore), then probed with α -*p16^{INK4a}* antibody (M-156).

The experimental cohort of *p16^{INK4a}* *TG* mice and littermate controls was generated after backcrossing two generations to C57Bl/6. Islet proliferation experiments were performed on progeny from *p16^{INK4a}*+/- intercrosses that had been backcrossed six or more generations to C57Bl/6. As *p16^{INK4a}*-deficient animals develop tumors with a median latency of 75 weeks¹, tumor-bearing animals were excluded from the analysis. All animals were housed and aged in the UNC barrier facility on standard diet. All animal work was approved and done in accord with the UNC Institutional Animal Care and Use Committee.

RNA preparation from islet and exocrine pancreas and qRT-PCR: Islets and exocrine pancreas were isolated from young (12-14 week) and old (64-80 week) mice by collagenase digestion followed by separation through centrifugation on a density gradient, as previously described in detail². RNA isolation, reverse transcription and TaqMan Real-time PCR were performed as described elsewhere³ with the exception that reverse transcription was performed using random hexamer rather than oligo-dT primer and more sensitive primer/probe sets specific for *p16^{INK4a}* and *Arf* were used (Supplemental Table 1). TaqMan analysis was performed on RNA isolated from islets and exocrine pancreas from four mice per indicated age group (Fig 1a, b; Supplemental Figure 1b,c).

Streptozotocin (STZ) treatment, glucose and insulin measurement: Cohorts of littermate mice of indicated ages and genotypes were weighed and treated after overnight fasting. STZ survival experiments were initially done in a cohort of FVB/n mice (backcrossed four generations); and were then repeated in two larger cohorts of C57Bl/6 mice (backcrossed 6 or more generations). Results did not differ between strains and were pooled for Kaplan-Meier analysis. STZ was dissolved in 10 mM ice cold sodium citrate buffer (pH 4.5) and immediately injected intraperitoneally as a single 150 mg/kg dose. Consistent with its known cytotoxic

effects, acute toxicity from STZ injection was observed prior to the onset of diabetes. Fifteen of 103 treated mice died within 5 days of injection. These acute deaths occurred independent of *p16^{INK4a}* genotype but were more frequent in animals aged 20-28 weeks than in younger animals. As these deaths occurred prior to the onset of hyperglycemia, they were censored from the analysis of diabetes-specific survival indicated in Figures 2b and 3a-c, although their inclusion does not alter the conclusions. Additionally, one *p16^{INK4a}-/-* mouse developed a soft tissue sarcoma at 25 weeks of age (96 days post-STZ) and was censored from the analysis. Weights and blood glucose concentrations were measured at weekly intervals after overnight fasting. Blood samples were taken from tail vein and blood glucose concentrations were measured with a home glucometer (Medisense Precision Xtra, Abbott Laboratories). For IP-GTT, cohorts of littermate female *p16^{INK4a} +/+* and *-/-* mice 17 to 52 weeks of age were fasted overnight followed by glucose injection (2 gm/kg body weight) as described^{2,4}. Serum glucose was measured at indicated times after the injection.

Immunohistochemistry and immunofluorescence: Assistance in sample processing was provided by the UNC Center for Gastrointestinal Biology and Disease and a commercial pathology lab (SR VetCheck). Comparison of proliferation between genotypes was performed by calculation of the Ki-67 (MIB1) proliferative index using well-established methods within the clinical laboratory at the Brigham and Women's Hospital Pathology Immunohistochemical laboratory. In brief, paraffin samples from indicated genetic backgrounds were fixed and processed in a uniform fashion. Five micron sections were cut and IHC staining for Ki-67 (Rabbit polyclonal, NCL-Ki67p, Novocastra) was performed using highly sensitive DAKO EnVision polymerized HRP detection methods. The proliferative index was calculated on a per islet basis as (Total Ki67+ islet cells)/(Total # of islet cells) per islet for each sample. Co-labeling

for insulin was performed on a subset of samples and demonstrated that >80% of proliferative Ki-67+ cells counted within islets were insulin+ β-cells. Positive (human tonsil) and negative controls (primary antibody omission on human appendix) were performed during all analyses. Pancreatic β-cells were identified by immunofluorescent staining for insulin (DAKO) with DAPI counterstain. For Ki-67/Insulin double labeling, sequential immunoperoxidase staining with mouse anti-human Ki-67 antibody (BD Pharmingen) and then guinea pig anti-bovine insulin antibody (Linco Research Inc.) was done with ABC kit. Color development was done as per the manufacturer's suggestions using Vector VIP substrate (Vector Laboratories Ltd) and DAB respectively.

Islet Analysis: To determine the kinetics of islet regeneration after STZ treatment, 10- to 12-week old C57/Bl6 mice were treated. To determine the influence of p16^{INK4a} expression on islet regeneration after STZ, littermate cohorts of 33-week old C57/Bl6 *p16^{INK4a}* +/+ and -/- mice were treated. Islet size was determined by photographing 15 to 30 islets from two mice for each time point after STZ treatment, and analyzing with Image-Pro express software. For analysis of islet proliferation with aging or post-STZ, pancreata were harvested and Ki-67 staining was performed as described on littermate pairs (either *p16^{INK4a}* +/+ and -/- or *p16^{INK4a}* TG and WT). For WT/TG young vs. old cohort N=6000 to 15,000 total islet cells comprising 31 to 127 islets were counted from 2 to 4 mice per genotype per age. For p16INK4a +/+ and -/- young vs. old cohort, N=8,500 to 40,000 total islet cells comprising 18 to 157 islets counted from 2 to 4 mice per genotype per age. For STZ-treated 33 week old *p16^{INK4a}* +/+ and -/- cohort of mice, N=2300 to 11,100 islet cells comprising 31 to 58 islets counted from 3 to 5 mice per genotype per time point. As islet proliferation and islet size were not normally distributed, statistical comparisons were made using a non-parametric (Mann-Whitney) test.

Legend to Supplementary Figures:**Supp. Figure 1: Real-Time quantitative PCR of islets and exocrine pancreas.**

- a. **Representative TaqMan tracings** of $p16^{INK4a}$ mRNA in purified islets of old (12 weeks) vs. young (64 weeks) mice (left). Representative TaqMan tracings of islet vs. exocrine pancreas of $p19^{ARF}$ (middle) and pdx (right) from old (64 week) mice. Thresholds for C_T determination are indicated.
- b. **mRNA expression data** of Figure 1a, graphed +/- standard error of the mean (SEM) on log2 scale.
- c. **mRNA expression data** of Figure 1b, graphed +/- standard error of the mean (SEM) on log2 scale.

Supp. Figure 2: $p16^{INK4a}$ BAC transgenic design and characterization.

- a. **Map** of BAC transgene and Southern probe.
- b. **Southern blot of two representative founder lines:** There is a variable microsatellite region near exon 1 α , producing a size difference in the C57Bl/6 (lane 3) and 129/SvEv (lanes 4 and 5) EcoR1 fragments. In the transgenic lines, the lower band represents the two-copy endogenous alleles from C57Bl/6, while upper band is from the 129/SvEv transgene. As the upper band is 50% the intensity of the lower band, both lines are single copy integrants.
- c. **TaqMan analysis:** Nine representative tissues were harvested as described from littermate pairs of 26 and 84 week old mice (2 littermate pairs per age). The ratio of expression in $p16^{INK4a}$ TG mice to wild-type littermates is plotted +/- SEM on a log₂ scale. The geometric mean across nine tissues is also indicated. As shown, $p16^{INK4a}$ expression was a mean 5.3 fold higher in $p16^{INK4a}$ TG mice compared to wild-type

littermates, while *Arf* expression was unaffected by the presence of the transgene.

Difference in expression between TG and WT mice was similar in young and old mice. “>” indicates expression in the WT allele below the level of detection.

Supp. Figure 3: p16^{INK4a} protein expression in BAC transgenic mice: Indicated tissues were harvested from a littermate pair of 75 week old *p16^{INK4a}* wild-type and BAC transgenic (TG) mice and analyzed for *p16^{INK4a}* expression by immunoprecipitation with α -*p16^{INK4a}* antibody followed by immunoblotting for *p16^{INK4a}*. Increased expression of *p16^{INK4a}* in tissues from transgenic mice compared to wild-type mice can be noted.

Supp. Figure 4: Weights and glucose tolerance in *p16^{INK4a}+/+ and -/-* mice by age.

- a. **Weights** of overnight fasted age- and sex-matched littermate *p16^{INK4a}+/+* versus *-/-* mice by age. N=10 to 14 mice per genotype per age. Results shown are +/- SEM.
- b. **Glucose tolerance in young and intermediate age *p16^{INK4a}+/+ and -/-* mice:**

Glucose tolerance was assayed through intraperitoneal glucose tolerance test (IP-GTT) in littermate *p16^{INK4a}+/+* and *-/-* mice of indicated ages. No effect of *p16^{INK4a}* nullzygosity was seen in 17-20 week animals (left graph). When a cohort of 40-52 week mice was tested, however, healthy *p16^{INK4a}* -deficient animals demonstrated a slight but significant ($p=0.019$, paired t-test) improvement in glucose tolerance relative to littermate controls (middle graph), but this effect was obscured by *p16^{INK4a}-/-* “outlier” animals that demonstrated persistent, severe hyperglycemia after IP glucose injection (right graph). Outlier animals were subsequently shown to harbor large splenic lymphomas which had not been evident on the day of IP-GTT. Therefore, functional analysis of the glucose-insulin axis in *p16^{INK4a}*-deficient mice

was limited by the tumor-prone condition of these animals, even in intermediate age (40-52 week old) mice.

Supp Figure 5: Islet regeneration post-streptozotocin

- a. **Percent Ki-67 positive cells** (dotted line, right y-axis) and islet size (box-whisker plot, left axis) on indicated day post-STZ. Islet size is shown indicating median, 25th to 75th percentile (boxes) and entire range (whiskers). *indicates p<0.02 for Ki-67 staining at indicated time points compared to day 0 time point. # indicates p=0.038 for islet size at day 8 compared to day 0.
- b. **Ki-67 (purple) and Insulin (brown) double labeling** on treated and untreated islet at indicated time point post-STZ. Original magnification X400.

Supp. Figure 6: Ki-67 immunohistochemistry positive and negative controls: As a measure of Ki-67 staining, positive and negative controls were included in each batch. Representative controls are shown: tonsil, a highly proliferative tissue, as a positive control (left) and appendix, a non-proliferative tissue, as a negative control (right). To maximize reproducibility, Ki-67 staining was performed using equipment and reagents that were certified for human clinical testing. Original magnification X200.

Supplementary Table:

List of newly designed primers and probes used for TaqMan Real-time quantitative PCR.

Murine Pdx-1 primer and probe sets were purchased from ABI. For all other primer sets, see Krishnamurthy et al³.

Murine Gene	Forward primer	Reverse primer	Probe (5'-FAM, 3'-Non Fluorescent Quencher)	Reference sequence
p16 ^{INK4a}	CGGTCGTACCCCGATT CAG	GCACCGTAGTTGAGCAGA AGAG	AACGTTGCCCATCATCA	AF044336
Arf	TGAGGGCTAGAGAGGGAT CTTGAGAAAG	GTGAACGTTGCCCATCAT CATC	ACCTGGTCCAGGATTC	NM_009877

References to supplementary information:

1. Sharpless, N. E., Ramsey, M. R., Balasubramanian, P., Castrillon, D. H. & DePinho, R. A. The differential impact of p16(INK4a) or p19(ARF) deficiency on cell growth and tumorigenesis. *Oncogene* 23, 379-85 (2004).
2. Montana, E., Bonner-Weir, S. & Weir, G. C. Beta cell mass and growth after syngeneic islet cell transplantation in normal and streptozocin diabetic C57BL/6 mice. *J Clin Invest* 91, 780-7 (1993).
3. Krishnamurthy, J. et al. Ink4a/Arf expression is a biomarker of aging. *J Clin Invest* 114, 1299-307 (2004).
4. Kulkarni, R. N. et al. Tissue-specific knockout of the insulin receptor in pancreatic beta cells creates an insulin secretory defect similar to that in type 2 diabetes. *Cell* 96, 329-39 (1999).